Advances in Astronomy and Space Physics, **8**, 24-27 (2018) doi: 10.17721/2227-1481.8.24-27

Metallicity calibrations and oxygen abundance evolution in massive galaxies

A. A. Maliuk[1]*, *I. A. Zinchenko*[2]

[1]Taras Shevchenko National University of Kyiv, Glushkova ave., 4, 03127, Kyiv, Ukraine
[2]Main Astronomical Observatory of the NAS of Ukraine, 27 Akademika Zabolotnoho Str., 03143 Kyiv, Ukraine

We determined oxygen abundances for the sample of SDSS galaxies with high masses using R_{3D}, S_{3D}, R_{2D}, S_{2D}, N and O3N2 calibrations. We investigated redshift–metallicity relation for oxygen abundances obtained by each calibration. We found that for galaxies with high stellar masses oxygen abundance obtained using all calibrations is increasing on the time interval from $z = 0.5$ to $z = 0$. However, the values of oxygen abundance enrichment rate significantly depend on adopted calibration and ranges from ~ 0.1 dex per unit redshift for R calibration to ~ 0.5 dex per unit redshift for O3N2 calibration.

Key words: ISM: H II regions – galaxies: abundances, evolution.

INTRODUCTION

Quantitative studies of oxygen abundance and its time evolution in the Universe is important for understanding the mechanisms of galaxies formation. However, precise estimation of the oxygen abundance in the galaxies at high redshift is a challenging task. It is impossible to use direct T_e method for calculation chemical abundance of distant galaxies as auroral lines, which are necessary to apply direct method, are too faint to be detected in spectra of these galaxies. Oxygen abundances calculated using strong lines methods (calibrations) also have large uncertainties up to 0.7 dex [7].

Previous studies have shown increasing of oxygen abundance with time. Kobulnicky [8] estimated the oxygen enrichment rate using R_{23} calibrations from KD02 and M91 as 0.14–0.19 dex per unit redshift for the sample of 204 galaxies at $z < 3$. Oxygen enrichment rate obtained by Lilly [11] with R_{23}-calibration appears to be significantly lower, about 0.08 ± 0.06 dex for over the last half of the age of the Universe. More recent study by Pilyugin [18] using C-method shows that oxygen enrichment rate depends on the galaxy mass: for galaxies with masses $10.25 < \log(M/M_{sun}) < 10.75$ it is 0.456 dex per unit redshift, for $10.75 < \log(M/M_{sun}) < 11.25$ – 0.325 dex, and for $11.25 < \log(M/M_{sun}) < 11.75$ – 0.250 dex. Thus, the value of the oxygen abundance rate is still under debate.

In this study we are going to examine oxygen enrichment rate during last few Gyrs using both well-known and recently developed calibrations.

Throughout the paper, we will be using the following notations for the line fluxes:

$$R_2 = [\mathrm{O\,II}]\lambda3727{+}\lambda3729 = I_{[\mathrm{O\,II}]\lambda3727+\lambda3729}/I_{\mathrm{H}\beta},$$

$$R_3 = [\mathrm{O\,III}]\lambda4959{+}\lambda5007 = I_{[\mathrm{O\,III}]\lambda4959+\lambda5007}/I_{\mathrm{H}\beta},$$

$$N_2 = [\mathrm{N\,II}]\lambda6548{+}\lambda6584 = I_{[\mathrm{N\,II}]\lambda6548+\lambda6584}/I_{\mathrm{H}\beta},$$

$$S_2 = [\mathrm{S\,II}]\lambda6717{+}\lambda6731 = I_{[\mathrm{S\,II}]\lambda6717+\lambda6731}/I_{\mathrm{H}\beta}$$

SAMPLE OF GALAXIES

We selected galaxies with measured fluxes of the emission lines [O II]$\lambda\lambda$3727,3729, [O III]$\lambda\lambda$4959,5007, [N II]λ6584, [S II]$\lambda\lambda$6717,6731, H_β ,H_α, redshifts and stellar masses from the Sloan Digital Sky Survey (SDSS DR12, [2]) We consider only galaxies with signal-to-noise ratio > 5 in each of lines listed above. We used photometric masses from SDSS DR12 database table `stellarMassStarformingPort` obtained by the Portsmouth method, which fits stellar evolution models to the SDSS photometry [12]. We used classical BPT-diagram [O III]λ5007/H_β – [N II]λ6584/H_α, suggested by Baldwin, Phillips and Terlevich [1] to separate spectra of H II regions from other emission-line objects. The positions of objects from our sample on the BPT diagram are shown in Fig. 1. Dashed line corresponds to dividing line between starforming and AGN-like objects suggested by Kewley [6]. Dividing line suggested by Kauffmann is shown by solid line [5]. H II regions lie below the dividing line. In this study we used more strict criteria for selecting H II regions suggested by Kauffmann [5].

*maliuk.andrey@ukr.net

Fluxes in emission lines were corrected for interstellar reddening using analytic approximation of Witford's interstellar reddening curve from the work [4]. The extinction coefficient $C_{\mathrm{H}\beta}$ was found using relation between intensities of lines H_β and H_α. Oxygen abundance calibrations obtained for low density H II regions. Thus, despite the fact that majority of extragalactic H II regions have low density, we adopt the intensity ratio [S II]λ6717/[S II]λ6731 as an electronic density indicator in H II regions [15] in order to select only low density objects. Using the condition $1.25 < F_{[\mathrm{S\,II}]\lambda6717}/F_{[\mathrm{S\,II}]\lambda6731} < 1.5$ we excluded objects with high electronic density and significant part of objects with unreliably measured lines.

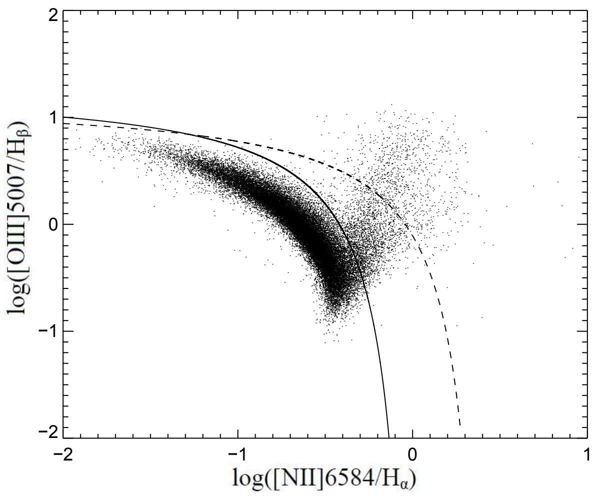

Fig. 1: BPT-diagram for our sample of SDSS galaxies. Dashed line corresponds to dividing line between starforming and AGN-like objects suggested by Kewley [6]. Dividing line suggested by Kauffmann is shown by solid line [5].

OXYGEN ABUNDANCES

We calculated oxygen abundance values $12 + \log(\mathrm{O/H})$ for each object of the sample using 6 calibrations. We apply two widely used calibration proposed by Pettini & Pagel [14]. N-calibration:

$$12 + \log(\mathrm{O/H}) = 8.90 + 0.57N2, \qquad (1)$$

where $N2 = \log([\mathrm{N\,II}]\lambda6584/\mathrm{H}_\alpha)$. And O3N2-calibration

$$12 + \log(\mathrm{O/H}) = 8.73 - 0.32O3N2, \qquad (2)$$

where

$$O3N2 = \log\left(([\mathrm{O\,III}]\lambda5007/\mathrm{H}_\beta)(\mathrm{H}_\alpha/[\mathrm{N\,II}]\lambda6584)\right).$$

Also, we will apply new calibrations developed by Pilyugin & Grebel [16], which based on the set of 313 H II regions with metallicities calculated using direct method. Three-dimensional R-calibration (hereafter R_{3D}-calibration):

$$12 + \log(\mathrm{O/H}) = 8.589 + 0.022\log(R_3/R_2) + \\ + 0.399\log N_2 + (-0.137 + 0.164\log(R_3/R_2) + \\ + 0.589\log N_2)\log R_2$$

if $\log N_2 < 0.6$ and

$$12 + \log(\mathrm{O/H}) = 7.932 + 0.944\log(R_3/R_2) + \\ + 0.695\log N_2 + (0.970 - 0.291\log(R_3/R_2) - \\ - 0.019\log N_2)\log R_2$$

if $\log N_2 \geq 0.6$. And three-dimensional S-calibration (hereafter S_{3D} - calibration):

$$12 + \log(\mathrm{O/H}) = 8.424 + 0.030\log(R_3/S_2) + \\ + 0.751\log N_2 + (-0.349 + 0.182\log(R_3/S_2) + \\ + 0.508\log N_2)\log S_2$$

for $\log N_2 < 0.6$ and

$$12 + \log(\mathrm{O/H}) = 8.072 + 0.789\log(R_3/S_2) + \\ + 0.726\log N_2 + (1.069 - 0.170\log\left(R_{/}S_2\right) + \\ + 0.022\log N_2)\log S_2$$

if $\log N_2 \geq 0.6$.

There are also two two-dimensional calibrations for the upper branch ($\log N_2 \geq 0.6$) have been proposed in [16]. Two-dimensional R-calibration (hereafter R_{2D}):

$$12 + \log(\mathrm{O/H}) = 8.589 + 0.329\log N_2 + \\ + (-0.205 + 0.549\log N_2)\log R_2$$

and two-dimensional S-calibration (hereafter S_{2D}):

$$12 + \log(\mathrm{O/H}) = 8.445 + 0.699\log N_2 + \\ + (-0.253 + 0.217\log N_2)\log S_2$$

REDSHIFT – METALLICITY RELATION

Oxygen abundance of a galaxy depends on its mass, redshift, starformation rate (SFR), environment, etc. [9, 17, 18]. However, mass–metallicity correlation is the most prominent and confirmed by many observations during several decades [3, 10, 19]. It should be noted that studies of the SDSS galaxies sample over a wide range of redshifts are often affected by selection effect. The sample of low-mass SDSS galaxies at high redshifts is incomplete due to severe difficulties with observations of such galaxies in the scope of this survey. Oxygen abundance of low-mass galaxies is also depends on SFR and environment [17, 18]. In order to avoid these effects we consider only massive galaxies. For that purpose we selected the subsample of SDSS galaxies with stellar masses $\log(M/M_{sun})$ higher than 10.25. This subsample contains 1700 objects. For this subsample we approximated the relation between metallicity and redshift z with function $12 + \log(\mathrm{O/H}) = az + b$ for each calibration. Coefficient a corresponds to the oxygen enrichment rate per redshift unit, b – oxygen abundance at $z = 0$. Values of the coefficients for oxygen abundance obtained with each calibration are presented in Table 1. Fig. 2 shows redshift–metallicity relation for our subsample. Triangles correspond to galaxies, solid lines represent an approximation of redshift–metallicity relation.

Table 1: Subsample of galaxies with stellar masses $\log(M/M_{sun}) \geq 10.25$.

Calibration	b	a	Err b	Err a
R_{3D}	8.597	−0.110	0.004	0.032
S_{3D}	8.627	−0.280	0.004	0.030
R_{2D}	8.626	−0.178	0.003	0.026
S_{2D}	8.630	−0.252	0.003	0.028
N	8.686	−0.149	0.003	0.021
$O3N2$	8.808	−0.496	0.005	0.041

For our subsample of galaxies with high masses we obtain the smallest value of enrichment rate $a = -0.110$ dex per unit redshift for R_{3D}-calibration and $a = -0.149$ for N-calibration. R_{2D} and both of S-calibrations provide intermediate values of a: −0.178, −0.280, and −0.252 dex, respectively. Maximum value of $a = -0.496$ dex was obtained for $O3N2$-calibration. Systematic errors of oxygen abundance enrichment rate are less than 0.05 dex in all cases.

The oxygen abundance for galaxies with high masses at $z = 0$ ranges from 8.597 dex for R_{3D}-calibration to 8.808 dex for $O3N2$-calibration. N-calibration also gives increased value of oxygen abundance of 8.686 dex. In paper [13] it was shown that there is danger of discrepancy between real oxygen abundance and one, calculated using ON-calibrations (without using of sulfur strong lines). But the unique correspondence disappears only for 5% of H II region models. Oxygen abundances calculated with S_{2D}, S_{3D} and R_{2D}-calibrations are well-agreed and are 8.630, 8.627 and 8.626 dex, respectively. It should be noted that S_{2D}-calibration is not based on usage of oxygen lines, but shows good agreement with three-dimensional calibrations, which take into account oxygen lines [16].

CONCLUSIONS

We determined oxygen abundances for the sample of galaxies with stellar masses $\log(M/M_{sun})$ higher than 10.25 using R_{3D}, S_{3D}, R_{2D}, S_{2D}, N, and $O3N2$-calibrations using sample of SDSS galaxies. We investigated redshift–metallicity relation for oxygen abundances obtained by each calibration.

We confirmed that for galaxies with stellar masses $\log(M/M_{sun}) > 10.25$ oxygen abundance is increasing on the time interval from $z = 0.5$ to $z = 0$ However, the values of oxygen abundance enrichment rate significantly depend on method of abundance calculation, i.e. adopted calibration. The minimal oxygen abundance enrichment rates, in range of $-0.1\ldots-0.2$ dex, were obtained for R_{3D}, R_{2D}, and N-calibrations. The higher values of oxygen enrichment rates, $-0.25\ldots-0.3$ dex, were obtained when using S_{3D} and S_{2D} calibration. Applying $O3N2$ calibration leads to the highest value of oxygen enrichment rate of almost −0.5 dex. We also obtained oxygen abundance for galaxies with high masses at $z = 0$, which is about 8.60 for R and S calibrations, ~ 8.7 for N-calibration, and ~ 8.8 for $O3N2$-calibration.

ACKNOWLEDGEMENT

Funding for SDSS-III[1] has been provided by the Alfred P. Sloan Foundation, the Participating Institutions, the National Science Foundation, and the U.S. Department of Energy Office of Science.

SDSS-III is managed by the Astrophysical Research Consortium for the Participating Institutions of the SDSS-III Collaboration including the University of Arizona, the Brazilian Participation Group, Brookhaven National Laboratory, Carnegie Mellon University, University of Florida, the French Participation Group, the German Participation Group, Harvard University, the Instituto de Astrofisica de Canarias, the Michigan State/Notre Dame/JINA Participation Group, Johns Hopkins University, Lawrence Berkeley National Laboratory, Max Planck Institute for Astrophysics, Max Planck Institute for Extraterrestrial Physics, New Mexico State University, New York University, Ohio State University, Pennsylvania State University, University of Portsmouth, Princeton University, the Spanish Participation Group, University of Tokyo, University of Utah, Vanderbilt University, University of Virginia, University of Washington, and Yale University.

[1] http://www.sdss3.org/

REFERENCES

[1] Baldwin J. A., Phillips M. M., Terlevich R. 1981, PASP, 93, 5.
[2] Eisenstein D. J., Weinberg D. H., Agol E. et al. 2011, AJ, 142, 72.
[3] Garnett D. R., Shields G. A. 1987, ApJ, 317, 82.
[4] Izotov Y. I., Thuan T. I., Lipovetsky V. A. 1994, ApJ, 435, 647.
[5] Kauffmann G., Heckmann T. M., Tremonti C. et al. 2003, MNRAS, 346, 1055.

[6] Kewley L. J., Dopita M. A., Sutherland R. S., Heisler C. A., Trevena J. 2001, ApJ, 556, 121.
[7] Kewley L. J., Ellison S. L. 2008, ApJ, 681, 1183.
[8] Kobulnicky H. A., Kewley L. J. 2004, ApJ, 617, 240.
[9] Lara-López M. A., López-Sanchez A. R., Hopkins A. M. 2013, ApJ, 764, 178.
[10] Lequeux J., Peimbert M., Rayo J. F., Serrano A., Torres-Peimbert S. 1979, A&A, 80, 155.
[11] Lilly S. J. & Carollo M. C., Stockton A. N. 2003, ApJ, 597, 730.
[12] Maraston C., Strömbäck G., Thomas D., Wake D. A., Nichol R. C. 2009, MNRAS, 394, 107.
[13] Melekh B. Ya., Pilyugin L. S., Korytko R. I. 2012, Kinematics and Physics of Celestial Bodies, 28, 189.
[14] Pettini M. & Pagel B. E. J. 2004, MNRAS, 348, 59.
[15] Pilyugin L. S. 2013, *Ionized gas in galaxies: physical state and chemical composition*, Naukova Dumka, Kyiv.
[16] Pilyugin L. S., Grebel E. K. 2016, MNRAS, 457, 3678.
[17] Pilyugin L. S., Grebel E. K., Zinchenko I. A., Nefedyev Y. A., Mattsson L. 2017, MNRAS, 465, 1358.
[18] Pilyugin L. S., Lara-López M. A., Grebel E. K. et al. 2013, MNRAS, 432, 1217.
[19] Skillman E. D. & Kennicutt R. C., Hodge P. W. 1989, ApJ, 347, 875.

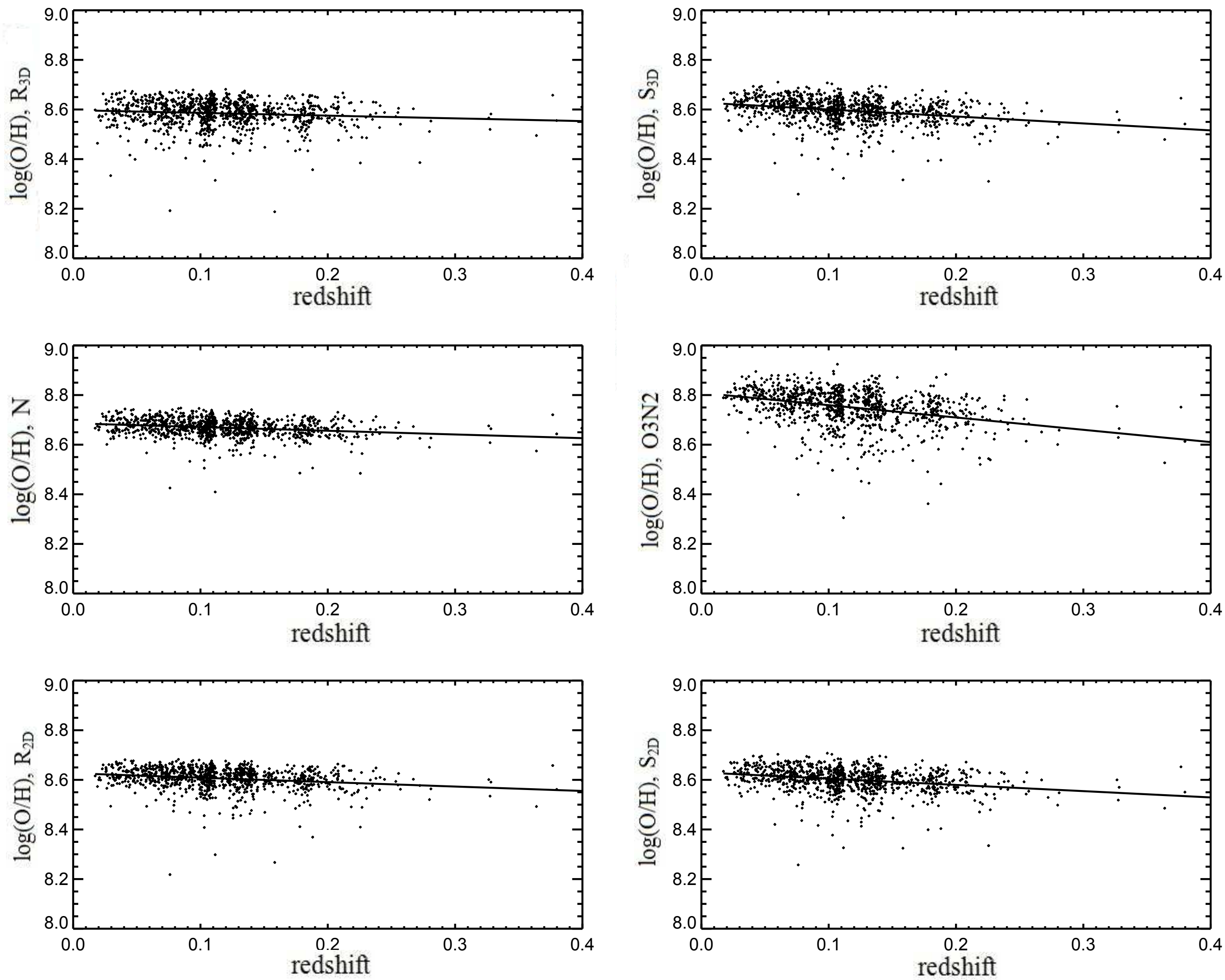

Fig. 2: Redshift–metallicity relations for the subsample of galaxies with stellar masses $\log(M/M_{sun}) \geq 10.25$. Metallicity calculated using R_{3D}, S_{3D}, R_{2D}, S_{2D}, N and $O3N2$-calibrations. Solid line represents the best-fit of the redshift–metallicity relation.